COSMOLOGICAL IMPLICATIONS OF MASSIVE NEUTRINOS

L.A. POPA

Institute for Space Sciences
R-76900 Bucharest - Măgurele, Romania

1. Introduction

The atmospheric neutrino results reported by the Super-Kamiokande [1] and MACRO [2, 3] experiments indicate that neutrinos oscillate, these data being consistent with $\nu_\mu \leftrightarrow \nu_\tau$ oscillations. The small value of the difference of the squared masses ($5 \times 10^{-4}\text{eV}^2 \leq \Delta m^2 \leq 6 \times 10^{-3}\text{eV}^2$) and the strong mixing angle ($\sin^2 2\theta \geq 0.82$) suggest that these neutrinos are nearly equal in mass as predicted by many models of particle physics beyond the standard model. Also, the LSND experiment [4] supports $\nu_\mu \leftrightarrow \nu_e$ oscillations ($\Delta m^2 \leq 0.2\text{eV}^2$); some solar neutrino experiments [5] suggest that ν_e could oscillate to a sterile neutrino $\nu_e \leftrightarrow \nu_s$ ($\Delta m^2 \simeq 10^{-5}\text{eV}^2$). The direct implication of neutrino oscillations is the existence of a non-zero neutrino mass in the eV range or lower, and consequently a not negligible hot dark matter (HDM) contribution $\Omega_\nu \neq 0$ to the total energy density of the universe. Recent works [6, 7, 8] show that the addition of a certain fraction of HDM component to the total energy density of the universe can lead to the agreement between the Cosmic Microwave Background (CMB) anisotropy power spectrum at the small scales and the observations of the Large Scale Structure (LSS) of the universe as derived by the redshift galaxy surveys [6].

The CMB anisotropy pattern contains information related to the physical processes occurring before the last scattering of the CMB photons; the LSS data reflects the clustering regime effects in our local universe. These measurements can provide independent probes for the structure of the universe on similar comoving scales at different cosmological epochs. This paper discusses the implications of massive neutrinos properties for CMB and LSS measurements.

2. Properties of the neutrino background

2.1. COSMOLOGICAL LIMITS ON NON-DEGENERATE NEUTRINO MASSES

Evidences has been accumulated that our universe is a low matter density universe (see e.g [9] and the references therein). Indications like the Hubble diagram of Type 1a supernovae and the acoustic peak distribution in the CMB anisotropy power spectra (see e.g. [10] and the references therein) point to a universe dominated by vacuum energy (cosmological constant Λ) that keeps the universe close to flat. The combined analysis of the latest CMB anisotropy data and Type 1a supernovae data indicates $\Omega_m = 0.25^{+0.18}_{-0.12}$ and $\Omega_\Lambda = 0.63^{+0.17}_{-0.23}$ [10] for matter and vacuum energy densities respectively, inferring a Hubble constant value of $H_0 \approx 65$ km s^{-1} Mpc^{-1} ($h = H_0/100$ km s^{-1}Mpc$^{-1} = 0.65$). Adding a HDM component to the ΛCDM model (ΛCHDM) leads to a worse fit to LSS data, resulting in a limit on the total non-degenerated neutrino mass of $m_\nu \leq 2$eV for a primordial scale invariant power spectrum and $m_\nu \leq 4$eV for a primordial scale free power spectrum [8]. A stronger upper limit is obtained from the matching condition of the LSS power spectrum normalization σ_8 (defined as the *rms* amplitude of the galaxy power spectrum in a sphere of radius $8h^{-1}$Mpc) at the COBE scale and at the cluster scale [9]. For the case of the ΛCHDM model having $\Omega_m = 0.3$, $\Omega_\Lambda = 0.7$ and a primordial scale invariant power spectrum it is found an upper limit of $m_\nu < 0.6$ if $H_0 < 80$ km s^{-1} Mpc^{-1}. Also, the constraints on the cosmological parameters obtained by using the most recent CMB anisotropy data [11] combined with Type 1a supernovae data implies a best fit model with $\Omega_m \approx 0.33$, Ω_Λ=0.67 and a neutrino density parameter $\Omega_\nu \approx 0.12$ ($\sum_i m_{\nu_i} \approx 92h^2\Omega_\nu = 4.66$eV) if priors H_0=65 km s^{-1} Mpc^{-1} and $\Omega_b h^2$=0.02 are assumed [12].

2.2. COSMOLOGICAL LIMITS ON NEUTRINO DEGENERACY

A way to improve the agreement of the cosmological models involving neutrinos with the higher values of Hubble parameter is to consider that neutrinos are degenerated. The neutrino degeneracy parameter ξ_ν is defined as $\xi_\nu = \mu_\nu/T_\nu$, where μ_ν is the neutrino chemical potential and T_ν is the neutrino temperature. The neutrino degeneracy enhances the contribution of the HDM component to the total energy density of the universe [13] changing the neutrino decoupling temperature [14], the abundance of light elements at the big bang nucleosynthesis (BBN) [15], the CMB anisotropies and the matter power spectrum [16]. Constraints on neutrino degeneracy coming from BBN [15] indicate $-0.06 \leq \xi_{\nu_e} \leq 1.1$ and $|\xi_{\nu_{\mu,\tau}}| \leq 6.9$. Bounds

on the neutrino degeneracy parameter are obtained by combining the current observations of the CMB anisotropies and LSS data [16]. The analysis of the CMB anisotropy data obtained by the Boomerang experiment indicates bounds on massless neutrino degeneracy parameter of $|\xi_{\nu_{e,\mu,\tau}}| \leq 3.7$, if only one massless neutrino species is degenerated, and $|\xi_\nu| \leq 2.4$, if the asymmetry is equally shared among three massless species [17].

2.3. MASSIVE NEUTRINO MIXING AND THE PHASE SPACE DISTRIBUTION FUNCTION

In the standard assumption of the mixing of massive neutrinos, the neutrino flavor eigenstates are described by a superposition of the mass eigenstate components that propagate differently with different energies, momenta and masses [21]. This paper considers two massive neutrino flavors ν_μ and ν_τ and a third neutrino flavor ν_e is massless. The mixing occurring in vacuum between ν_μ and ν_τ can be written as:

$$\begin{aligned} |\nu_\mu\rangle &= \cos\theta_0|\nu_2\rangle + \sin\theta_0|\nu_3\rangle \\ |\nu_\tau\rangle &= -\sin\theta_0|\nu_2\rangle + \cos\theta_0|\nu_3\rangle, \end{aligned} \tag{1}$$

where ν_2 and ν_3 are the mass eigenstate components and θ_0 is the vacuum mixing angle. It is usual to consider that each neutrino of a definite flavor is dominantly one mass eigenstate [21]. In this circumstance, the dominant mass eigenstate component of ν_μ is ν_2, that of ν_τ is ν_3 and their difference of the squared masses is $\Delta m^2 = m_3^2 - m_2^2$.

In the expanding universe, the system of neutrinos drops out from thermal equilibrium with $e^\pm$, photons, the small fraction of baryons and other massive species (e.g. $\mu^+\mu^-$ pairs) when the ratio of the averaged weak interaction rate to the expansion rate falls below unity. The present values of neutrino temperature T_{ν_0} and the present temperature of the CMB photons $T_0 \approx 2.725$K are related through $T_{\nu_0}/T_0 \simeq (3.9/g_{*D})^{1/3}$, where g_{*D} is the number of degrees of freedom in equilibrium at neutrino decoupling. For a degeneracy parameter $\xi_\nu \leq 15$ the neutrino decoupling temperature is of few MeV [14] and from the entropy conservation one obtains that after decoupling $T_{\nu_0} \simeq (4/11)^{1/3} T_0$. It follows that the total degeneracy parameter ξ_ν is conserved and the present lepton asymmetry of the neutrino background is [15]:

$$L_\nu = \frac{1}{12\zeta(3)} \frac{T_{\nu_0}}{T_0} [\xi_\nu^3 + \pi^2 \xi_\nu],$$

where $\zeta(3)$ is the Riemann function of 3. At decoupling, neutrino with mass in eV range behave like a relativistic particle and its full phase space

distribution function can be written as a pure Fermi-Dirac distribution function $f^0_\nu(q)$, a zero-order distribution that depends only on momenta, plus a perturbed part $\Psi(\mathbf{x},\mathbf{q},a)$ that depends on momenta, position and time [22]:

$$f_\nu(\mathbf{x},\mathbf{q},a) = f^0_\nu(q)(1+\Psi(\mathbf{x},\mathbf{q},a)) \qquad f^0_\nu(q) = \frac{1}{\mathrm{e}^{E_\nu/T_\nu \pm \xi_\nu}+1}\,, \tag{2}$$

where: $E_\nu = \sqrt{q^2+a^2m^2_\nu}$ is the neutrino energy, a is the cosmological scale factor ($a_0 = 1$ today), q is the comoving neutrino momentum, $\pm\xi_\nu$ is the neutrino(-sign)/antineutrino(+sign) degeneracy parameter and m_ν is the dominant mass component. The full neutrino phase space distribution function was computed through numerical simulations [23] based on the standard particle-mesh (PM) method. The initial neutrino positions and velocities was generated from the HDM matter density fluctuation power spectrum by using Zel'dovich approximation [24]. Figure 1 shows (left panels) the contour plots of the constant particle probabilities in δq-$\delta\rho_{HDM}$ plane, where δq is the fluctuation of the neutrino comoving momentum and $\delta\rho_{HDM}$ is the fluctuation of the neutrino density field. It is also shown (right panels) the momentum distribution functions obtained from numerical simulations (continuous line) compared with a pure Fermi-Dirac distribution function (dashed line). The time evolution of the phase space distributions f_{ν_μ} and f_{ν_τ} of ν_μ and ν_τ can be written as [25]:

$$\begin{aligned}
\partial f_{\nu_\mu}(\mathbf{x},\mathbf{q},t)/\partial t &= -<\mathcal{P}>_{\nu_\mu} f_{\nu_\mu}(\mathbf{x},\mathbf{q},t) + <\mathcal{P}>_{\nu_\tau} f_{\nu_\tau}(\mathbf{x},\mathbf{q},t),\\
\partial f_{\nu_\tau}(\mathbf{x},\mathbf{q},t)/\partial t &= -<\mathcal{P}>_{\nu_\tau} f_{\nu_\tau}(\mathbf{x},\mathbf{q},t) + <\mathcal{P}>_{\nu_\mu} f_{\nu_\mu}(\mathbf{x},\mathbf{q},t),
\end{aligned} \tag{3}$$

where: $<\mathcal{P}>_{\nu_\mu}$ and $<\mathcal{P}>_{\nu_\tau}$ are the neutrino mixing probabilities, $dt = da/(aH)$ and H is the Hubble expansion rate:

$$H^2 = \frac{8\pi G}{3}[\Omega_m/a^3 + \Omega_r/a^4 + \Omega_\Lambda + \Omega_k/a^3]. \tag{4}$$

In the above equation G is the gravitational constant, $\Omega_m = \Omega_b + \Omega_{cdm} + \Omega_\nu$ is the matter energy density parameter and Ω_b, Ω_{cdm}, Ω_ν are the energy density parameters for baryons, cold dark matter and neutrinos, Ω_r is the energy density parameter for radiation (including photons and one relativistic neutrino flavor), Ω_Λ is the vacuum energy density parameter and $\Omega_k = 1-\Omega_m-\Omega_\Lambda$ is the energy density parameter related to the curvature of the universe. The set of equations (3) assume that, apart from the neutrino mixing, no other physical processes take place, leading to the conservation of total neutrino number densities n_ν and degeneracy parameters ξ_ν. It follows that non-vanishing mixing and degeneracy parameters would lead to changes of the energy density, pressure, their perturbations, the shear

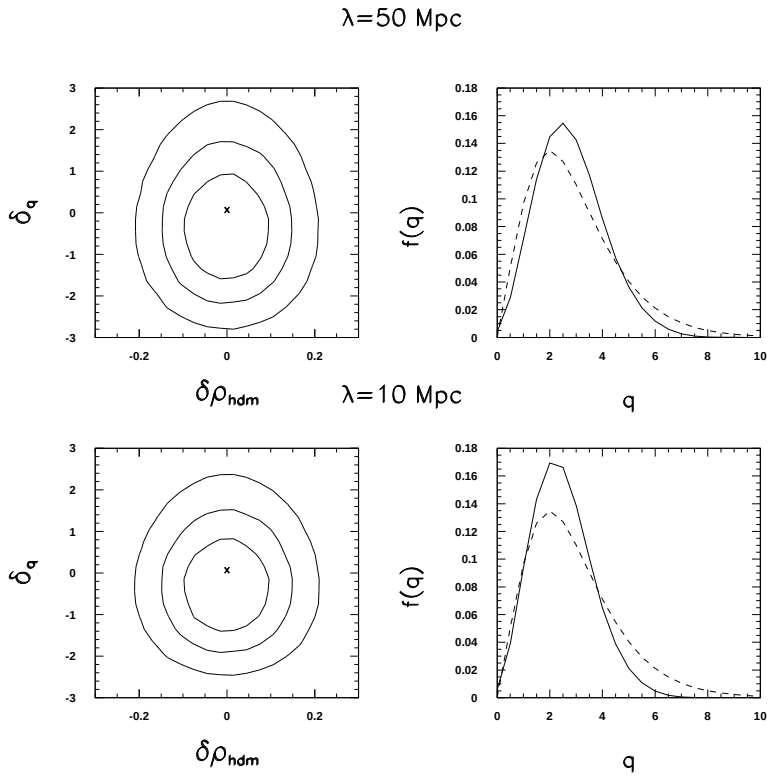

Figure 1. Left panels: the contour plots of constant particle probabilities in the $\delta q - \delta\rho_{HDM}$ plane. From exterior to interior the contours correspond to: 0.75, 0.5 and 0.25 probability. Right panels: the full neutrino phase space distribution functions obtained from numerical simulations (continuous line) and the pure Fermi-Dirac distribution function (dashed line).

stress and the energy flux of each massive neutrino flavor, quantities that are related to the neutrino phase space distribution function [25]. Figure 2 presents the time evolution of the energy density parameters and of the density perturbations of different components (matter, radiation, vacuum, neutrinos) for few values of neutrino mixing and degeneracy parameters. One can observe that the variation of Δm^2 and $\Delta\xi_\nu$ affect the energy density parameters and the density perturbations for all components, while the variation of $\sin^2 2\theta_0$ affect only the neutrino density perturbations, reflecting the conservation conditions imposed by equations (3).

3. CMB temperature and matter density fluctuations

During the epochs where the anisotropies are generated, neutrinos with masses in eV range can have significant interactions with the photons,

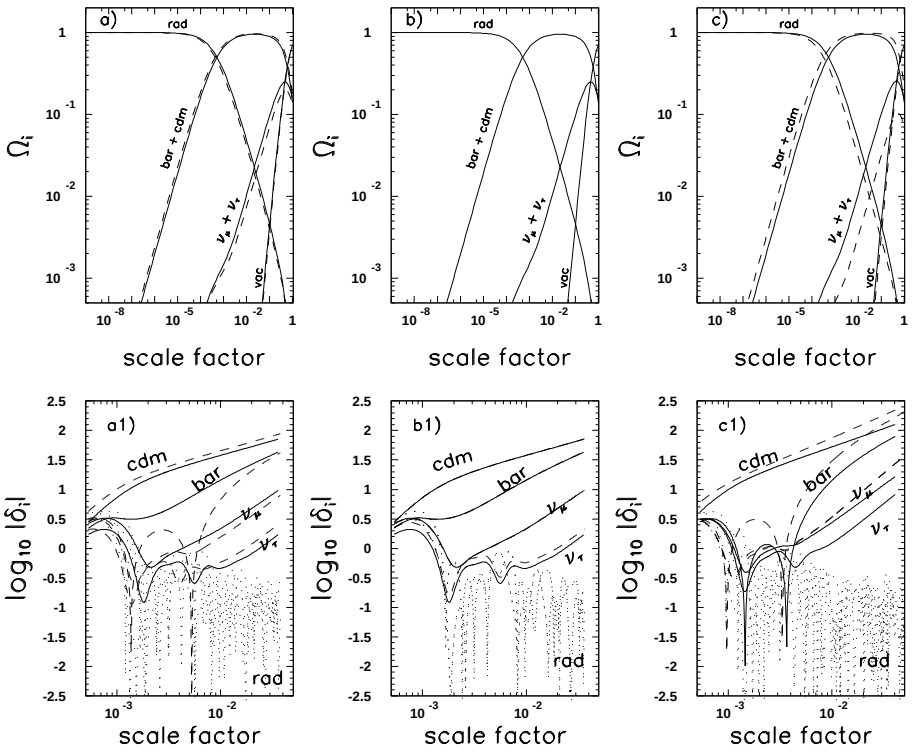

Figure 2. The evolution with the scale factor of the energy density parameters Ω_i and of the density perturbations δ_i of the various components in a ΛCHDM model having $\Omega_b = 0.023$, $\Omega_\Lambda = 0.67$, $\Omega_m = 0.33$, $h = 0.65$, $m_\nu = m_{\nu_\mu} + m_{\nu_\tau} = 0.6$eV and $\xi_\nu = \xi_{\nu_\mu} + \xi_{\nu_\tau} = 5$. (a) and (a1): $\sin^2 2\theta_0 = 0.8$, $\Delta\xi_\nu = 4$, $\Delta m^2 = 0.24\text{eV}^2$ (continuous line) and $\Delta m^2 = 0.18\text{eV}^2$ (dashed line). (b) and (b1): $\Delta m^2 = 0.24\text{eV}^2$, $\Delta\xi_\nu = 4$, $\sin^2 2\theta_0 = 1$ (continuous line) and $\sin^2 2\theta_0 = 0.45$ (dashed line). Panels (c) and (c1): $\Delta m^2 = 0.24\text{eV}^2$, $\sin^2 2\theta_0 = 0.45$, $\Delta\xi_\nu = 4$ (continuous line) and $\Delta\xi_\nu = 2$ (dashed line).

baryons and cold dark matter particles only via gravity. Thus differences introduced by the neutrino mixing of the phase space distributions and the lepton asymmetry of the neutrino background are due to the differences in the gravitational field of the neutrinos. As it was shown in the previous section, the neutrino energy density and pressure as well as the perturbed the energy density and pressure, the shear stress and energy flux are modified by the mixing of the neutrino degenerated background. They determine differences in the equation of state of massive neutrinos ($w = p_\nu/\rho_\nu$), in the expansion law of the universe (eq. 4) and originate the metric perturbations affecting the growth of fluctuations in other components.

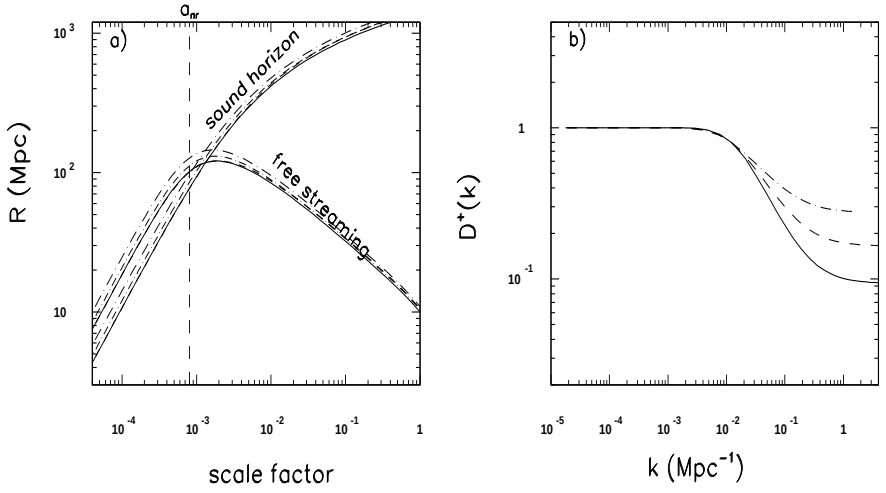

Figure 3. (a): The dependence of the time evolution of neutrino free streaming distance and sound horizon distance on Δm^2 and $\Delta\xi_\nu$ when: $\Delta m^2 = 0.24\text{eV}^2$ and $\Delta\xi_\nu = 4$ [$\Omega_\nu = 0.16$] (continuous line), $\Delta m^2 = 0.2\text{eV}^2$ and $\Delta\xi_\nu = 4$ [$\Omega_\nu = 0.15$] (dashed line), $\Delta m^2 = 0.24\text{eV}^2$ and $\Delta\xi_\nu = 1$ [$\Omega_\nu = 0.07$] (dash-dotted line). The vertical line indicates the approximated value of the scale factor when massive neutrinos start to make the transition from radiation to matter. (b): The growth functions of the perturbations at the present time ($z = 0$) obtained for: $\Delta m^2 = 0.24\text{eV}^2$ and $\Delta\xi_\nu = 4$ [$\Omega_\nu = 0.16$] (continuous line), $\Delta m^2 = 0.2\text{eV}^2$ and $\Delta\xi_\nu = 4$ [$\Omega_\nu = 0.15$] (dashed line), $\Delta m^2 = 0.24\text{eV}^2$ and $\Delta\xi_\nu = 1$ [$\Omega_\nu = 0.07$] (dash-dotted line). The cosmological model is a flat ΛCHDM model having: $\Omega_b = 0.023$, $\Omega_\Lambda = 0.67$, $\Omega_m = 0.33$, $h = 0.65$, $m_\nu = m_{\nu_\mu} + m_{\nu_\tau} = 0.6\text{eV}$ and $\xi_\nu = \xi_{\nu_\mu} + \xi_{\nu_\tau} = 5$.

3.1. THE NEUTRINO GRAVITATIONAL INFALL

Characteristic to the cosmological models involving massive neutrinos is the scale-dependence of the growth rate of perturbations. Neutrinos can cluster via gravitational instabilities only on distances below a characteristic distance, the free streaming distance, analogous to the Jeans scale of self-graviting systems (see e.g. [22] and the references therein).
The neutrino free streaming distance is related to the causal horizon distance $\eta(a)$ through [26]:

$$R_{fs} = \frac{1}{k_{fs}} = \frac{\eta(a)}{\sqrt{1 + (a/a_{nr})^2}}, \quad \eta(a) = \int_0^a \frac{da}{a^2 H}, \tag{5}$$

where: k_{fs} is the free streaming wave number, a is the cosmological scale factor, H is the Hubble expansion rate given by the equation (4) and a_{nr} is the scale factor when massive neutrinos start to become non-relativistic

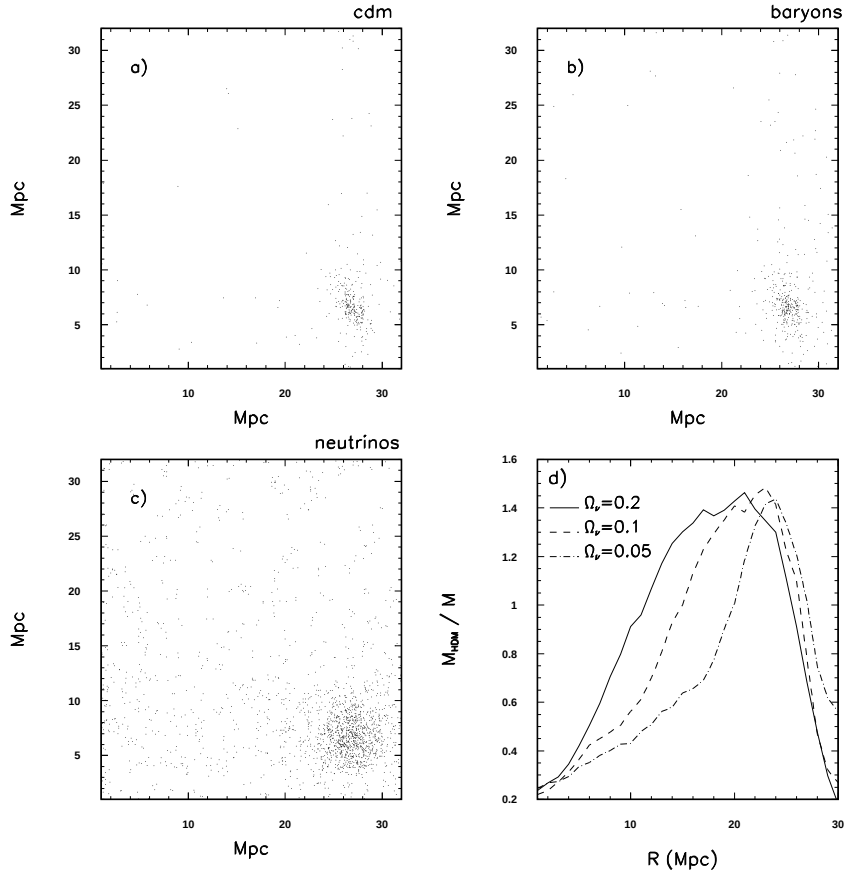

Figure 4. Maxima of the mass distribution of the cold dark matter component (panel a), baryonic component (panel b) and hot dark matter component (panel c) obtained from numerical simulations of 32^3 particles in a box of size 32 Mpc for the ΛCHDM model [$\Omega_b = 0.023$, $\Omega_\Lambda = 0.67$, $\Omega_m = 0.33$, $h = 0.65$, $m_\nu = m_{\nu_\mu} + m_{\nu_\tau} = 0.6$eV and $\xi_\nu = \xi_{\nu_\mu} + \xi_{\nu_\tau} = 5$]. Panel d): The mass distribution of the HDM component obtained from numerical simulations for different neutrino fractions (see also the text). The total mass in all simulations is $M = 2.27 \times 10^{15} M_\odot$.

$(a_{nr} = (1 + z_{nr})^{-1} \approx 3k_B T_{\nu_0}/m_\nu c^2)$.
Another important scale is given by the sound horizon distance of the baryon-photon fluid defined as [26]:

$$R_s = \int_0^{\eta(a)} c_s(a) d\eta, \quad c_s^2(a) = \frac{1}{3} \frac{1}{1 + \frac{3}{4} a \frac{\Omega_\gamma}{\Omega_b}}, \tag{6}$$

where: $c_s(a)$ is the sound speed and Ω_γ and Ω_b are the energy density parameters of photons and baryons at the present time. Panel a) in Figure

3 presents the dependence of time evolution of the neutrino free streaming distance and sound horizon distance on Δm^2 and $\Delta\xi_\nu$. Panel b) of the same figure shows the evolution with the wave number of the growth functions of perturbations obtained for the same values of these parameters. The increase of Δm^2 when $\Delta\xi_\nu$ is kept constant leads to the increase of Ω_ν and of z_{nr}. The same effect is obtained when Δm^2 is kept constant and $\Delta\xi_\nu$ is increased. At early times, when neutrinos are relativistic, the free streaming distance is approximately the sound horizon distance. After the neutrinos become non-relativistic, the free streaming distance decreases with time becoming smaller than the sound horizon distance. Also, the growth of perturbations is suppressed at smaller scales, the magnitude of the suppression depending on neutrino parameters.
It follows that neutrinos can cluster gravitationally on increasingly small scales at latter times, damping the amplitude of the density perturbations. This implies that the characteristics of the cosmological structures at small redshift, as the mass density profile and the velocity dispersion profile of clusters, can probe the neutrino properties. Figure 4 presents maxima of the mass distribution of the cold dark matter component, the baryonic component, and the hot dark matter component, obtained from numerical simulations in a flat ΛCHDM model. The cold dark matter and the baryonic matter components accrete the hod dark matter component via gravity. The gravitational potential governing this process is given by the Poisson equation $\nabla^2\Phi = 4\pi G a^2 \bar{\rho}\epsilon_m(k,a)$, where $\bar{\rho} = \Omega_m \rho_{cr}$ is the averaged density, ρ_{cr} is the critical density and $\epsilon_m(k,a)$ is the net perturbation of the density field. Also, panel d) of the Figure 4 presents the mass distribution of the HDM component (obtained for each simulation bin and normalized to the total mass of each bin) for different neutrino fractions.

3.2. CMB ANISOTROPY AND THE MATTER POWER SPECTRA

In the linear perturbation theory, the CMB anisotropy and matter transfer function are computed by the integration of coupled and linearized Einstein, Boltzmann and fluid equations [22] that describe the time evolution of the metric perturbations in the perturbed density field and the time evolution of the density fields for all the relevant particles. Figure 5 presents the dependence of the CMB anisotropy power spectra (left panels) and matter density fluctuations power spectra (right panels) on the neutrino difference of the squared masses Δm^2, the mixing angle $\sin^2 2\theta_0$ and the lepton asymmetry L_ν [25]. For all cases it is assumed a total neutrino mass $m_\nu = m_{\nu_\mu} + m_{\nu_\tau} = 0.6\text{eV}$ and a total neutrino degeneracy parameter $\xi_\nu = \xi_{\nu_\mu} + \xi_{\nu_\tau} = 5$. The CMB power spectra are normalized to COBE/DMR four-Year data and the matter density fluctuations power spectra are nor-

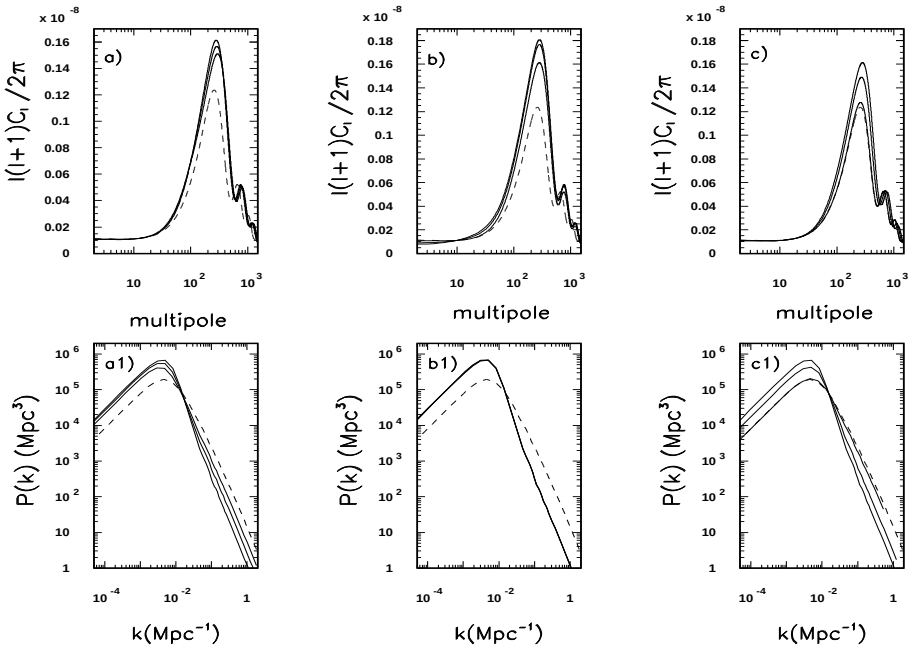

Figure 5. The CMB anisotropy power spectra and the matter density fluctuations power spectra. Panels a) and a1): $\sin^2 2\theta_0 = 0.8$, $\Delta\xi_\nu = 4$ and (from top to bottom) Δm^2=0.24, 0.2, 0.01 eV^2. Panels b) and b1):$\Delta m^2 = 0.24$eV^2, $\Delta\xi_\nu = 4$ and (from top to bottom) $\sin^2 2\theta_0$=1, 0.8, 0.45. Panels c) and c1):$\Delta m^2 = 0.24$eV^2, $\sin^2 2\theta_0$=0.8 and (from top to bottom) $\Delta\xi_\nu$=4, 3, 1. In each panel are presented (dashed lines) the power spectra obtained in the same cosmological model when $\Delta m^2 = 0$, $\Delta\xi_\nu = 0$ and $\sin^2 2\theta_0 = 0$.

malized to the abundance of the rich clusters at the present time [23].
The CMB anisotropy power spectra show two distinct features: a vertical shift of the C_l at large l (present in all panels) with the increasing of Δm^2, $\sin^2 2\theta_0$ and $\Delta\xi_\nu$ values, that results from the modification of neutrino free streaming scales, and an horizontal shift of the Doppler peaks to lower l when Δm^2 and $\Delta\xi_\nu$ are increased, that results from the increase of the sound horizon at recombination. The horizontal shift of C_l is not present in panel b1) because the variation of $\sin^2 2\theta_0$, when Δm^2 and $\Delta\xi_\nu$ are fixed, does not change Ω_ν and consequently the Hubble expansion rate is not changed. The matter density fluctuations power spectra reflects the same features: the increasing of Δm^2 and $\Delta\xi_\nu$ values results in the modification of neutrino free streaming scales and consequently a suppression of the growth of fluctuations on all scales below the free streaming scale ($k_{fs} \simeq 0.02\mathrm{Mpc}^{-1}$). By using the Fisher information matrix method it was found [25] that the future high precision CMB experi-

ments as PLANCK surveyor will permit to detect a lepton asymmetry of the neutrino background $Ł_\nu \geq 4.5 \times 10^{-3}$, a difference of the neutrino squared masses $\Delta m^2 \geq 9.7 \times 10^{-3}\text{eV}^2$ and a mixing angle $\sin^2 2\theta_0 \geq 0.13$. Also, the combined data from PLANCK and Sloan Digital Sky Survey will permit the determination of the total neutrino mass $m_\nu \geq 3 \times 10^{-2}\text{eV}$, with any prior information on cosmological parameters [23].

4. Conclusions

The standard Cold Dark Matter model has difficulties in matching the CMB and LSS measurements. Cosmological models involving a mixture of CDM and HDM particles, the CHDM models, are able to fit, the excess large scale power seen in galaxy surveys and the CMB temperature fluctuations.

The results from neutrino oscillation experiments indicate a non-zero neutrino mass in the eV range, or lower. This implies a non-negligible contribution of neutrinos to the total energy density of the universe. The experimental evidence indicating a present low matter density universe, dominated by the vacuum energy ($\Omega_m \simeq 0.3$, $\Omega_\Lambda \simeq 0.7$) and a higher Hubble parameter value ($H_0 \simeq 65$ km s^{-1}Mpc^{-1}) are in agreement with cosmological models involving neutrinos if one considers the lepton asymmetry of the neutrino background.

At the times when the anisotropies were generated, neutrinos had significant interactions with the photons, baryons and cold dark matter particles only via gravity. Neutrinos can not cluster via gravitational effects on scales k below the free streaming scale $k < k_{fs}$ (large wavelengths). For $k > k_{fs}$ the growth of the density perturbations is suppressed, the magnitude of this suppression depending on Ω_m, Ω_ν, Δm^2 and $\Delta\xi_\nu$.

The neutrino homogeneous quantities (density and pressure) and inhomogeneous quantities (density and pressure perturbations, the shear stress and the energy flux) are also changed in the presence of non-degenerated neutrino mixing, leaving imprints on the CMB temperature fluctuations and the matter density fluctuations power spectra.

The determination of the fundamental cosmological parameters with high precision CMB and LSS surveys requires complementary knowledge of neutrino properties from cosmic rays and long base-line experiments.

Acknowledgements: I acknowledge the organizers and V. Berezinsky for useful discussions during this workshop.

References

1. Fukuda, Y. *et al.* (Super-Kamiokande Coll.) (1998) Evidence for oscillation of atmospheric neutrinos, *Phys. Rev. Lett.* **81** 1562

2. Ambrosio, M. *et al.* (MACRO Coll.) (1998) Measurement of the atmospheric neutrino-induced upgoing muon flux using MACRO, *Phys. Lett.* **B434** 451
3. Ambrosio, M. *et al.* (MACRO Coll) (2000) Low energy atmospheric neutrinos in MACRO, *Phys. Lett.* **B478** (2000) 5
4. Athanassopoulos, C. et al. (1998) Results on $\nu_\mu \rightarrow \nu_e$ Neutrino Oscillations from the LSND Experiment, Phys. Rev. Lett. **81**, 1744
5. Bahcall, J.N., Krastev, P.I. & Smirnov, A.Yu. (1998) Where do we stand with solar neutrino oscillations?, Phys. Rev. **D** 58, 096016
6. Primack, R.J., Holtzman, J., Klypin, A., Caldwell, D.O. (1995) Cold +Hot Dark Matter Cosmology with $m_{\nu_\mu} \approx m_{\nu_\tau} \approx 2.4$eV, *Phys. Rev. Lett.* **74** 12 2160
7. Silk, J. & Gawiser, E. (1998) From the Cosmological Microwave Background to Large-Scale Structure, *Science* **280** 1405
8. Gawiser, E. (2000) Limits on neutrino masses from large-scale structure, astro-ph/0005475
9. Fukugita, M., Liu, G.C., Sugiyama, N. Limits on neutrino mass from Cosmic Structure Formation, (1999) Phys. Rev. Lett. **84**, 1082
10. Efstathiou, G., Bridle, S.L., Lasenby, A.N., *et al.* (1999) Constraints on Ω_Λ and Ω_m from Distant Type 1a Supernovae and Cosmic Microwave Background Anisotropies, *MNRAS* **303** L47-52
11. Jaffe, A.H. *et al.* (2000) Cosmology from MAXIMA-1, Boomerang & COBE/DMR CMB Observations, astro-ph/000733
12. Tegmark, M., Zaldarriaga, M. (2000) Current cosmological constraints from a 10 parameter CMB analysis, astro-ph/0002091 v2
13. Larsen, G.B. & Madsen, J. (1995) Mixed dark matter with neutrino chemical potential, *Phys. Rev.* **D** 52 4282
14. Freese, K. *et al.* (1983) Massive, degenerate neutrinos and cosmology, *Phys. Rev.* **D** 27 1689
15. Kang, H. & Steigman, G. (1992) Cosmological constraints on neutrino degeneracy, *Nucl. Phys.* **B** 372 494
16. Kinney, W.H. & Riotto, A. (1999) Measuring the Cosmological Lepton Asymmetry through the CMB Anisotropy, *Phys. Rev. Lett.* **83** 3366
17. Hannestad, S. (2000) New constraints on neutrino physics from Boomerang data, astro-ph/0105220
18. Pal, P.B. & Kar, K. (1999) How degenerate can cosmological neutrino be?, *Phys. Lett.* **B** 451 136
19. Lesgourgues, J. & Pastor, S. (1999) Cosmological implications of a Relic Neutrino Asymmetry, *Phys. Rev.* **D** 60 103521
20. Lesgourgues, J., Pastor, S. & Prunet, S.(1999) Cosmological measurement of neutrino mass in the presence of leptonic asymmetry, hep-ph/9912363
21. Particle Data Group (1998) The Europ. Phys. J. **C3**, 1.
22. Ma, C.P., Bertschinger, E. (1995) Cosmological Perturbation Theory in the Synchronous and Conformal Newtonian Gauge, *ApJ* **455** 7
23. Popa, L.A., Burigana, C., Mandolesi, N. (2001) Cosmological parameter determination from PLANCK and SDSS data in ΛCHDM cosmologies, *ApJ* **558** 10
24. Zel'dovich, Ya.B. (1970) Gravitational Instability: An Approximate Theory for Large Density Perturbations, *A&A* **5** 84
25. Popa L.A., Burigana, C., Finelli, F., Mandolesi, N. (2000) On the detection of neutrino oscillations with PLANCK surveyor, *A&A* **363** 825
26. Dodelson, S., Gates, E., Stebbins, A. (1996) Cold+Hot Dark Matter and the Cosmic Microwave Background, *ApJ* **467** 10
27. Jenkins, A., Frenk, C.S., Pearce, F.R. *et al.* (1998) Evolution of structure in cold dark matter universe, *ApJ* **499** 20